Materials Science & Engineering A 616 (2014) 20–28

Contents lists available at ScienceDirect

Materials Science & Engineering A

journal homepage: www.elsevier.com/locate/msea

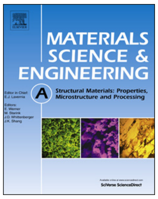

Effects of processing optimisation on microstructure, texture, grain boundary and mechanical properties of Fe–17Cr ferritic stainless steel thick plates

Jian Han [a,*], Huijun Li [a], Zhixiong Zhu [a], Laizhu Jiang [b], Haigang Xu [b], Li Ma [b]

[a] School of Mechanical, Materials and Mechatronic Engineering, University of Wollongong, Wollongong, NSW 2522, Australia
[b] Baoshan Iron & Steel Co., Ltd., Shanghai 200431, China

ARTICLE INFO

Article history:
Received 15 June 2014
Received in revised form
29 July 2014
Accepted 30 July 2014
Available online 7 August 2014

Keywords:
Ferritic stainless steel
Thick plate
Processing optimisation
Microstructure
Mechanical property

ABSTRACT

The relationships between microstructure, texture, grain boundary and tensile strength, Charpy impact toughness of (Nb+Ti+V) stabilised Fe–17Cr ferritic stainless steel thick plates were investigated by means of optical microscopy, X-ray diffraction, scanning electron microscopy, electron backscatter diffraction, tensile and Charpy impact testing. The results show that for Fe–17Cr ferritic stainless steel thick plate, the addition of warm rolling procedure leads to refinement of grain size, modification of texture, and then optimisation of grain boundary, including grain boundary character distribution and grain boundary connectivity. Meanwhile, the mechanical testing results indicate that optimal transformation that warm rolling procedure brings to Fe–17Cr ferritic steel thick plate is beneficial to its mechanical properties.

1. Introduction

Ferritic stainless steel (FSS) with body centred cubic (BCC) structure is essentially Fe–Cr or Fe–Cr–Mo alloy [1]. FSS has various advantages in comparison with austenitic stainless steel (ASS): lower cost, higher thermal conductivity, smaller linear expansion and better resistance to chloride stress-corrosion cracking, atmospheric corrosion and oxidation. Due to these merits, FSS is very attractive in various application fields [2–4]. The Fe–17Cr FSS, together with stabilising additions, such as Nb, V, Ti, is considered to be a significant candidate to replace ASS [5].

However, the limitation of Fe–17Cr FSS is its relatively high ductile to brittle transition temperature (DBTT) [6], which is usually above room temperature, particularly for thickness beyond 5 mm [7]. At present, Fe–17Cr FSS thick plates (above 4 mm) have been applied in many industrial fields. The challenge of Fe–17Cr FSS thick plate is to improve toughness properties, maintain tensile properties, and utilise the other attributes of this steel group.

The toughness property of FSS, which is comparatively lower than that of the other stainless steel grades, is related to the BCC structure. For BCC crystallography, it is unavoidable to limit numbers of available slip systems, lower the deformation compatibility and increase the probability of initiation and propagation of brittle fracture [8]. The crack cores formed at the boundaries of deformation bands cause brittleness of FSS [9]. It is extensively accepted that coarse grains tend to promote crack initiation, and thus the grain size mainly contributes to resistance to initiation of brittle fracture and slightly to crack propagation.

The microstructure, texture and grain boundary, which are influenced during processing modification, have a close correlation with properties, especially mechanical properties of steels [10,11].

The influences of microstructure, such as grain refinement, on mechanical properties of materials have been studied by a quantity of researchers. Then, crystalline texture can strongly affect grain boundary misorientation, leading to the change of coincidence site lattice (CSL), which is used by classifying grain boundaries [12]. It has been recognised that grain boundary engineering (GBE) plays an important role in controlling mechanical properties of materials [13], such as strength and ductility. In GBE, grain boundary character distribution (GBCD) and grain boundary (GB) connectivity have shown a close correlation with these properties [12,14]. GBE involves a series of thermomechanical treatments designed to convert a fraction of the high-energy grain boundaries (random boundaries) to low-energy boundaries, which are identified as low-Σ CSL boundaries (CSLBs), including low-angle boundaries (LABs) [15]. The CSL model is employed to describe GBCD by classifying grain boundaries as low-Σ CSLBs ($\Sigma \leq 29$ and $\Delta\theta \leq 15^\circ \Sigma^{-1/2}$) [16] and high-$\Sigma$ CSLBs ($\Sigma > 29$, random boundaries) [15]. Here, the Σ is the reciprocal density of coincident sites at the grain boundaries

---

* Corresponding author. Tel.: +61 405427056; fax: +61 242213238.
E-mail address: jh595@uowmail.edu.au (J. Han).

http://dx.doi.org/10.1016/j.msea.2014.07.107
0921-5093/

between two adjoining grains. Among the low-Σ CSLBs, Σ1 (i.e. LABs) and Σ3 are usually the dominant boundaries.

Thermomechanical processing (TMP), using single or multiple steps of deformation and subsequent annealing treatment, has been one of the most popular approaches applied for the modification of microstructure, texture, GBE [17], and finally mechanical properties. During TMP, warm working is frequently applied for the modification of grain, texture and grain boundary [18].

In this study, the traditional hot rolling process of (Nb+V+Ti)-stabilised Fe–17Cr FSS thick plate was optimised to investigate the role of intermediate warm rolling procedure on microstructure, texture, grain boundary and then mechanical properties of the studied steels. Different total reductions for warm rolling processes were selected for comparison with the traditional one, and enhancing effect of properties was assessed.

2. Experimental work

2.1. Materials and manufacturing processes

The Fe–17Cr FSS used in this study was melted in a vacuum induction furnace. The casting ingots were hot forged into the thickness of 26 mm (traditional and first optimised hot rolling process) and 35 mm (second optimised hot rolling process), hot rolled into 5.5 mm plate, and annealed at high temperatures for corresponding duration, aiming at sufficient recrystallisation and fine annealing microstructure, followed by cooling in water. The chemical composition of the Fe–17Cr steel is shown in Table 1. The stabilisation ratio (the ratio of stabilising elements and interstitial elements, i.e. (Nb+V+Ti)/(C+N)) of the studied steel is 23.6. The result means the designed steel can satisfy the requirements of intergranular corrosion resistance [19–21].

Two different warm rolling processes are selected during hot rolling to compare with the traditional hot rolling process, and the detailed processing parameters and reductions of each pass are displayed in Table 2. The total reductions of three rolling processes are 78.8%, 78.8% and 84.3%, respectively, and the reductions of each stage are exhibited in Table 3.

2.2. Phase calculation

The equilibrium phase diagrams were calculated using Thermo-Calc software based on TCFE6 database, and the recommended temperature range is from 500 to 1600 °C. The details of phases were illustrated by the scale of Y axis ranged from 0 to 1 mol and 5×10^{-3} mol.

Table 1
Chemical composition (wt%) of the studied Fe–17Cr steel.

C	Si	Mn	Cr	Nb	V	Ti	N	Fe
0.005	0.19	0.28	17.0	0.04	0.12	0.10	0.006	Bal.

2.3. Microstructure analysis

As-annealed specimens for microstructural analysis were cut, prepared according to the standard metallographic procedures, and then etched in the etchant containing 5 g Cu_2SO_4, 20 ml hydrochloric acid (HCl) and 20 ml H_2O. The longitudinal section of specimen was observed using optical microscopy (OM) of Zeiss Axioplan 2. The grain sizes were measured by computer programme using planimetric method.

2.4. Texture

The textures formed at different hot rolling processes were measured by using X-ray diffraction (XRD) on a Bruker D8 discover diffractometer with Co-K_α radiation, and orientation distribution functions (ODFs) $f(g)$ were calculated by the series expansion method according to Bunge (the maximum expansion degree, $l_{max}=22$) from three incomplete pole figures {1 1 0}, {2 0 0} and {1 1 2}.

2.5. Grain boundary

To further characterise the microstructure, scanning electron microscopy (SEM) and electron backscatter diffraction (EBSD) were performed using a JEOL JSM 7001F field emission gun (FEG) SEM. Prior to EBSD mapping, the specimens were electro-polished in a A_3 solution at 50 V for 90 s. The low-Σ CSLB and GB connectivity were interpreted by using the software Channel 5 based on the EBSD results.

2.6. Tensile strength and impact toughness testing

Tensile tests were performed at room temperature with strain rate of $5 \times 10^{-3}\ s^{-1}$. The transverse yield strength (YS, 0.2% proof stress), ultimate tensile strength (UTS) and elongation were measured. The Charpy testing was conducted in the temperature range from −40 to 60 °C, employing sub-size (5 mm × 10 mm × 55 mm) specimens. All Charpy specimens were prepared with the longitudinal direction that parallels to the rolling plane. A 2 mm deep Charpy V-notch was cut through the thickness direction perpendicular to the rolling plate. The testing standard is ASTM A370 [22], ASTM E8/E8M [23] and ASTM E23 [24].

Table 3
Pass distribution of three studied hot rolling processes.

Steel no.	Process	Hot rolling reduction (%)	Warm rolling reduction (%)
T#	Traditional hot rolling	78.8	–
P1#	Warm rolling-1	53.8	54.2
P2#	Warm rolling-2	53.1	66.5

Table 2
Comparison of three studied hot rolling processes.

Steel no.	Process	Hot rolling procedure		Warm rolling procedure		Final annealing procedure
		Temperature range (°C)	Intermediate thickness (mm)	Warm rolling temperature (°C)	Final thickness (mm)	Temperature/time (°C/min)
T#	Traditional hot rolling	850–1100	–	–	5.5	900/7
P1#	Warm rolling-1	850–1100	12	260	5.5	850/5.5
P2#	Warm rolling-2	850–1100	16.4	260	5.5	850/5